Tree Physiology 40, 5–18
doi:10.1093/treephys/tpz092

Methods paper

Embolism resistance of different aged stems of a California oak species (*Quercus douglasii*): optical and microCT methods differ from the benchtop-dehydration standard

R. Brandon Pratt[1,2], Viridiana Castro[1], Jaycie C. Fickle[1] and Anna L. Jacobsen[1]

[1]Department of Biology, California State University, Bakersfield, 9001 Stockdale Hwy, Bakersfield, CA 93311; [2]Corresponding author (rpratt@csub.edu)
http://orcid.org/0000-0001-7537-7644

Received April 13, 2019; accepted August 15, 2019; handling Editor Marilyn Ball

Vulnerability of xylem to embolism is an important trait related to drought resistance of plants. Methods continue to be developed and debated for measuring embolism. We tested three methods (benchtop dehydration/hydraulic, micro-computed tomography (microCT) and optical) for assessing the vulnerability to embolism of a native California oak species (*Quercus douglasii* Hook. & Arn.), including an analysis of three different stem ages. All three methods were found to significantly differ in their estimates, with a greater resistance to embolism as follows: microCT > optical > hydraulic. Careful testing was conducted for the hydraulic method to evaluate multiple known potential artifacts, and none was found. One-year-old stems were more resistant than older stems using microCT and optical methods, but not hydraulic methods. Divergence between the microCT and optical methods from the standard hydraulic method was consistent with predictions based on known errors when estimating theoretical losses in hydraulic function in both microCT and optical methods. When the goal of a study is to describe or predict losses in hydraulic conductivity, neither the microCT nor optical methods are reliable for accurately constructing vulnerability curves of stems; nevertheless, these methods may be useful if the goal of a study is to identify embolism events irrespective of hydraulic conductivity or hydraulic function.

Keywords: conductivity, drought, embolism, HRCT, hydraulics, *Quercus*, water relations.

Introduction

Plants transport water under negative pressure, and this leads to a characteristic risk of transport failure. When tissues dehydrate, such as occurs during a drought, gas may be pulled into xylem conduits and fill them, which leads to gas blockages known as emboli (Davis et al. 2005). Emboli diminish the hydraulic conductivity of the xylem and, if extensive, can lead to mortality of organs and entire plants (Pratt et al. 2008, Kursar et al. 2009). Species widely differ in their resistance to embolism, and understanding the role of embolism resistance in drought tolerance is a research priority for vegetation modeling (Mackay et al. 2015).

There has been debate about methodologies to quantify resistance to embolism formation and, in particular, the use of centrifuge-based methods to generate negative pressures. This debate has been extensively discussed elsewhere (Cochard et al. 2015, Hacke et al. 2015). There are two methods that generally yield reliable results. One, the benchtop-dehydration method dehydrates large branches on a benchtop, stems are periodically and carefully removed from the branch and their level of embolism is quantified by measuring hydraulic conductivity. With this method, the negative pressures in the xylem develop much the same as they would in an intact plant. Moreover, smaller stems can be cut from the branches and yield reliable estimates of embolism levels (Torres-Ruiz et al. 2015, Venturas et al. 2016). This method also has the advantage that it directly measures the hydraulic conductivity of the xylem, thus quantifying the effect of embolism on the movement of water through the complex vascular system of a plant. This is important because this is the simplest way to account for

the many factors that affect the conductivity of xylem tissue, such as the hydraulic resistances of pit membranes, perforation plates and the presence of non-functional but not embolized conduits (Jacobsen and Pratt 2018, Pratt and Jacobsen 2018). This method is not without challenges, and difficulties may arise when working with cut stems that should be tested (Choat et al. 2010, Jacobsen and Pratt 2012, Venturas et al. 2016).

Another method that has been argued to yield reliable results is X-ray scanning using micro-computed tomography systems (microCT). In this method, organs are scanned with tissue-penetrating X-rays and images are captured to construct 3D models of the vascular system. This method can distinguish between gas-filled conduits that are embolized compared with fluid-filled ones; however, identifying which of the fluid-filled conduits are hydraulically conductive requires additional methods (Pratt and Jacobsen 2018). MicroCT methods have the same advantage of the benchtop method in that negative pressures in the plants can develop as they do in vivo. A further advantage is that fully intact plants can be sampled when grown in containers. A limitation of this method is that it does not directly measure hydraulic conductivity, but instead quantifies the number of conduits that are fluid-filled. Theoretical hydraulic conductivity can be estimated by measuring conduit diameters and calculating it using the mathematical description of flow through an ideal conduit (the Hagen–Poiseuille equation); however, this calculation can lead to errors because plant conduits are not ideal tubes and their diameters change along their length, which violates a requirement of meeting the Hagen–Poiseuille ideal. Moreover, plant conduits have pit membranes that must be crossed, which is not factored into the calculation (Schulte et al. 1987). Finally, the influence of these factors is likely not uniform across vascular networks that differ anatomically and as they experience embolism during dehydration (Jacobsen and Pratt 2018, Mrad et al. 2018).

Another more recently developed method for measuring embolism resistance is referred to as the optical method. This method, when applied to stems, involves peeling back a section of bark to expose the xylem so that it can be photographed. The xylem is photographed as the plant dehydrates using a scanner or a camera and the occurrence of embolism events is observed in the images over time along with xylem pressure measurements. The plant is dehydrated to extreme negative pressures, and the total number of observed events is tallied. The percentage of events can be calculated from the time series of images and plotted against xylem pressure potential to generate a vulnerability curve. One limitation of this method with stems is that it is typically only possible to measure a small amount of xylem tissue. Another is that debarking the stems can lead to damage in the sampled area (Venturas et al. 2019). Due to these limitations and the relative newness of this method, further testing at this stage is valuable (Brodribb et al. 2017).

Using the optical method, Skelton et al. (2018) reported that various oak species were highly resistant to embolism. They suggested that numerous other reports which have found that oaks were more vulnerable than what they found could be accounted for by the ring-porous nature of oak xylem, coupled with relatively long vessels reported for some oak species, and the use of flawed methods to construct some vulnerability curves. However, the conclusions of Skelton et al. (2018) have limitations. They sampled only current year stems of oaks, which are generally diffuse porous (Gilbert 1940, Rodriguez-Zaccaro et al. 2019, Rosell et al. 2017), and ring-porosity does not develop until later years. This makes their ring porosity explanation difficult to interpret because many previous studies were conducted on older stems that would indeed be ring or semi-ring porous, which differs from their study. A second limitation of the Skelton et al. (2018) study is that they did not compare the optical method to other methods and the other studies that they claim to be in error did not use the optical method. Thus, it is possible that there are methodological differences between the relatively untested optical method compared with other methods that could explain the discrepancy between their findings and previously published reports.

In the present study, we examined vulnerability to embolism of one of the oak species that Skelton et al. (2018) examined. We chose to sample *Quercus douglasii* because it was the most embolism-resistant oak species they sampled. We tested two critical issues that were not included in Skelton et al. (2018): we examined the vulnerability to embolism of different stem ages (1-, 2- and 3-year-old stems), and we compared three independent methods used to examine stem vulnerability to embolism including benchtop dehydration, microCT and optical methods.

Materials and methods

Field site

Blue oak (*Quercus douglasii* Hook. & Arn., Fagaceae) was sampled at a field site in Bakersfield (35°21′20″ N, 119°06′13″ W), CA, USA. The region is a desert (<150 mm of annual rainfall) with a Mediterranean-type rainfall pattern. All measurements were made between August and October 2018. The weather over this time period was hot and dry during the day and cool at night. High temperatures were between 25 and 40 °C, and the low temperature was 10 °C. No rain fell during the sampling period. The trees were growing on the edge of a wildland area just upland from the Kern River in an area known as the Kern River Environmental Studies Area. Nearby native plants, closer to the river than our plants, included Fremont cottonwood (*Populus fremontii*), Goodding's willow (*Salix gooddingii*) and mule fat (*Baccharis salicifolia*).

This study site was ideal for our work for two reasons. First, it is about 0.25 km from our laboratory; thus, samples could

be processed quickly. Second, the plants were irrigated by an automated drip-watering system that watered the plants daily, which meant that the plants were not exposed to water deficits prior to our experiments. To verify this, we measured predawn water potential of plants on 7 and 10 September 2018 using a pressure chamber (Model 2000, PMS Instrument Company, Albany, OR, USA) to assess their water status. The first time we sampled, measurements were taken just before dawn on branchlets from each tree (n = 4 reps per plant). Sampling at predawn meant that the leaves, branches, stems, roots and soil would be in equilibrium so we would have an estimate of stem pressure potential. However, the values from this sampling were more negative than expected, which we hypothesized was due to nighttime transpiration. Thus, we again measured on 10 September after bagging branchlets overnight with locking plastic bags covered in aluminum foil to halt nighttime transpiration. This approach allowed us to measure maximum stem water potential, but because we did not bag entire trees, our samples likely did not equilibrate with soil water potential.

We intensively sampled three mature individual trees, each about 8 m in height. This was done because the chief goals of the study were to compare stems of different ages and to compare different methods for constructing vulnerability curves. All three methods were used on all three trees. Stem age was assessed by visually locating terminal bud scale scars, and stem age was later confirmed on samples by making cross sections and counting annual growth rings.

Vessel length

Maximum vessel lengths were measured for 3-year-old stems using a standard air-injection method and an injection pressure of 100 kPa (Greenidge 1952). Maximum vessel length was sampled to inform our sampling methods (see below).

We sampled mean vessel length for all ages. Branches were cut underwater from hydrated trees at predawn in the field and transported to the laboratory with their cut ends underwater. In the lab, different-aged stem segments were excised underwater from the larger collected branches. Basal stem ends were attached to a tubing system and were injected at 50 kPa for 24 h with a two-component silicone (Rhodorsil RTV-141, Rhodia USA, Cranbury, NJ, USA) containing a UV stain (Uvitex OB, Ciba Specialty Chemicals, Basel, Switzerland) dissolved in chloroform (1% by weight). To determine the vessel length distribution from the silicone-injection point, cross sections were obtained from the silicone-injection point (0.0 cm) and 0.7, 1.4, 2.9, 5.8 and 11.8 cm from the injection point. For each section, fluorescent micrographs were taken (Zeiss SteREO Discovery.V12 with AxioCam HRc digital camera, Carl Zeiss Microscopy, LLC, Thornwood, NY, USA). All silicone-filled vessels were counted at each sampled distance. The mean vessel length was calculated from these counts using the equations reported by Sperry et al. (2005).

Vulnerability to embolism curves using three methods

For all three methods, plant material was sampled in the same way. Large branches (2–2.5 m long) were cut from the plants in the field and brought back to the laboratory. These samples were collected around dawn when plant xylem pressures were at their least negative. Long branches were cut so that the sampled stems were >1.5 m away from where the cut was made (see maximum vessel length data in Results). Cut ends of branches were immediately submerged in water and were transported to the nearby laboratory in ≤5 min. Once in the laboratory, stems were recut under water and allowed to hydrate for about 2 h, after which their water potentials were about −0.2 MPa.

For dehydration treatments, large branches were double-bagged, and the branches were equilibrated for at least 1.5 h (often much longer) prior to sampling water potential using a pressure chamber. To further dehydrate samples, large branches were removed from the bags for a time and then again re-bagged to equilibrate. This process was repeated, using many large branches, so that we sampled across a wide range of water potentials. Water potentials were measured on three or more branchlets, with more samples for when variation was greater (a 0.2-MPa difference between maximum and minimum). Bagging and equilibrating samples was an important step so that leaves were not transpiring and were equilibrated with stems to accurately estimate stem xylem pressure.

Stems were sampled from the larger branch by cutting it under water about 20 cm away from the target stem. After the initial cut underwater, the cut portion of the stem sat in water for about 5 min to minimize negative pressures. The stem was then successively cut shorter until it was the target length (14 cm). This procedure has been shown to avoid cutting artifacts (Venturas et al. 2016; see Supplemental material available as Supplementary Data at *Tree Physiology* Online for tests).

For microCT vulnerability curves, the apical portion of the shoot was left intact and the cut portion was submerged in water in a 1- to 3-ml plastic container. Leaves were plastic-wrapped around the stems. Scanned shoots were about 40–50 cm tall. Stems were marked on their bark with a gold paint pen so that they could later be rescanned in the exact same location (gold can be easily seen in scans). Scans were done by rotating the sample 180° at rotation steps ≤0.3°. Scans took between 5 and 16 min, depending on exact settings, with most taking 11 min. The X-ray source was set at 40 or 50 kV and 600 μA (SkyScan model 2211, Bruker Corporation, Billerica, MA, USA). Scan resolution was 3–5 μm. Once scanned, images were aligned and reconstructed using InstaRecon software (InstaRecon, Champaign, IL, USA). All samples were scanned intact to image the number and diameter of all embolized conduits using CTAn Software (CTAn, Bruker microCT, Bruker

Corporation, Billerica, MA, USA). After a stem was scanned and hydraulic conductivity was measured (see below), it was cut to approximately 2 cm length, with the gold marked region included in this section, and injected with dry air at 50–100 kPa for 5 min to dehydrate it. This was done because it is easy to distinguish gas-filled conduits since gas absorbs very little X-rays compared with the surrounding fluid-filled cells and cell walls. This allowed us to estimate the number of non-embolized conduits in fresh samples (total conduits in dried sample minus the embolized conduits in fresh samples). In total, 44 stems were sampled across the three age classes using microCT and these stems were approximately evenly sampled across the three trees (Tree 1 $n = 15$, Tree 2 $n = 15$, Tree 3 $n = 14$).

Embolism level was estimated by calculating theoretical (t) conductivity (K_t) losses. Theoretical specific conductivity (K_{ts}) was calculated from microCT-measured conduit diameters (D, m) using the Hagen–Poiseuille relationship and the cross-sectional area of stems (A):

$$\text{Theoretical specific conductivity } (K_{ts}) = \frac{\sum(D^4\pi)}{128\eta * A} * \rho_{water}\,(\text{kg m}^{-1}\,\text{s}^{-1}\,\text{MPa}^{-1}) \quad (1)$$

In this relationship, η is the viscosity of water ($9.532 * 10^{-10}$ MPa s) and ρ_{water} is the density of water (997.7 kg m^{-3}), both at 22 °C. K_t was also calculated with Eq. (1), without the A term. To make K_{ts} comparable to measured hydraulic values, measurements were adjusted to 22 °C. To estimate theoretical PLC from the microCT data (PLC_t), the native-state embolism was estimated by first calculating the K_t of total number of conduits in air-dehydrated fresh samples (K_{tmax}) and subtracting the K_t of embolized conduits (K_{te}) in native-state samples. This yielded native state $K_t = K_{tmax} – K_{te}$. Loss of theoretical hydraulic conductivity (%) could then be calculated as

$$PLC_t = (1 - K_t/K_{tmax}) * 100 \quad (2)$$

For benchtop hydraulic vulnerability curves (the benchtop or hydraulic method), samples were measured by feeding solution into stems at low pressure and then measuring the outflow using an analytical balance (CP124s, Sartorius, Göttingen, Germany). In most cases, stems were measured for conductivity following sampling in the microCT system and we sampled the same portion of the stem that was scanned ($n = 12$ for 1- and 3-year old; $n = 19$ for 2-year old). To do this, immediately after scanning, stems were cut to length (8–14 cm) under water and cut ends were trimmed with fresh razor blades. Stems had already been partially cut down for microCT measurements, so this step only involved cutting off the tops of these hydrated shoots. Stems were mounted in the conductivity system and fed a 20-mM KCl solution that was filtered with a 0.1 µm pore exclusion filter and degassed using a membrane contactor (Liqui-Cel mini-module; Membrana, Charlotte, NC, USA). The pressure head was kept low to avoid displacing emboli (2–3 kPa). Outflow was collected on a balance and recorded every 10 s by a computer attached to the balance. Flow rate was taken as the mean of steady-state flow over 40 s. Flow was measured in the absence of a pressure head before and after the pressurized flow measurement, the two values averaged and subtracted from the measured flow rate (Hacke et al. 2000), which enables measurements to be accurately made even when flow is not fully steady-state. Flow rate, pressure head and stem length were all used to calculate hydraulic conductivity of stems (kg m s^{-1} MPa^{-1}). Following measuring initial conductivity (K_h), emboli were removed by flushing stems for 60 min at 100 kPa. Conductivity maximum (K_{hmax}) was measured following the flush. Conductivity was expressed as a percentage of maximum (percentage loss of hydraulic conductivity, PLC_h) where

$$PLC_h = (1 - K_h/K_{hmax}) * 100 \quad (3)$$

Otherwise, conductivity was divided by stem area and expressed as stem area-specific conductivity (kg m^{-1} s^{-1} MPa^{-1}), which is directly comparable to microCT K_{ts} estimates (Eq. (1)). Total sample sizes for hydraulic measurements were $n = 24$ for 1-year old, $n = 23$ for 2-year old and $n = 17$ for 3-year old stems.

When measuring K_h using the hydraulic method, solution is pushed through all the vessels in the xylem that are not permanently occluded by blockages, such as tyloses. In samples >1-year-old, the hydraulic method will represent a bulk measurement of all growth rings. For this reason, we measured conduits in all growth rings with microCT, so that they would be comparable to the hydraulic data.

Vulnerability to embolism was measured using the optical method (Brodribb et al. 2017). To do this, large branches were collected from the field as with the other methods. The branches were bagged with cut ends in water for about 2 h prior to the onset of measurements. Twenty-four mega pixel digital cameras (Fujifilm XT-2 and E3, Fujifilm Corporation, Tokyo, Japan) with macro lenses (Fujinon XF80 mm f/2.8 or the Mitakon Creator 20 mm f/2, Zhyong Yi Optics, Shenyang City, China) were set up to image a small portion of xylem from 1-, 2- and 3-year-old stems ($n = 3$ for each age). To view the xylem, a small rectangle of bark (about 0.4 cm^2) was carefully removed with a fresh razor blade while keeping the cut area moist. After the xylem was exposed, a layer of silicone grease was spread on the cut area to prevent water loss. Preliminary experiments found severe dehydration and shrinkage if the silicone grease was not added. The cameras photographed the xylem every 2–5 min. The plant was then dehydrated over the course of 2–2.5 days, and water potential of branchlets were measured using a pressure chamber between 9 and 16 times. After initial testing, nine

measurements, taken at key points, was found to be sufficient to produce a polynomial fit with r^2 values >0.98. Branches and branchlets were individually bagged so that some bags could be removed to allow dehydration over time while other branches remained bagged. Bagged branchlets were used to estimate stem pressure potential with a pressure chamber. Overnight, all foliar area was bagged to prevent excessive dehydration.

Photographs were made into time-lapse videos that were 1 frame per second (Photoshop CC, Adobe, San Jose, CA, USA). BatchPhoto software (BatchPhoto, Bit&Coffee Ltd, Craiova, Romania) was used to date and time stamp each image. Videos were watched and 'optical events' were recorded along with the date and time. Optical events could be matched with a particular stem pressure potential by the date/time stamp. Measured xylem-pressure values were plotted over time and fit with a polynomial that allowed us to calculate pressure potential at any time during the drydown. This procedure was done for every branch sampled. The optical events were summed over the duration of the dry down, and the percentage of the maximum was calculated and plotted against pressure potential to create a vulnerability curve. The target minimum pressure potential was −7 MPa as our preliminary measurements indicated that PLC = 100% by that point.

Evaluating functional xylem of different-aged stems

MicroCT cannot directly identify conduits that are actively transporting sap. Developing conduits or ones blocked by water-rich compounds or structures, such as gums and tyloses, may appear as fluid-filled and interpreted as functional in images. We tested which conduits were functional by feeding an iodine-rich compound (iohexol) into the transpiration stream in a transpiring plant. After uptake, we scanned the stem to assess the distribution of iodine in the samples to evaluate which vessels were functional (see methods in Pratt and Jacobsen 2018).

Testing for artifacts: validation of hydraulic-based methods

We tested for artifacts related to cutting, X-ray exposure, clogging, re-filling and flushing in a series of experiments that are described in the Supplemental material available as Supplementary Data at *Tree Physiology* Online, and reported in the Results.

Analyses

Vulnerability curves were fit with two-parameter Weibull curves, and the xylem pressures at 10, 50 and 75% loss of conductivity (P10, P50 and P75, respectively) were extracted from curves. For the hydraulic and microCT data, bootstrapping was used to calculate 95% confidence limits (Hacke et al. 2015; R 3.5.1). For the optical curves, three different stems from three different individuals were used to calculate P10, P50 and P75. No curve fit was necessary because the curves created a continuum (Figure S1 available as Supplementary Data at *Tree Physiology* Online). We chose P10 as representing the onset of embolism, P50 as the commonly reported midpoint and P75 as an endpoint where plants are in danger of mortality (Kursar et al. 2009). Stem ages were compared by assessing means and overlap between confidence limits. Differences among methods were assessed using a mixed-model ANOVA that included treatment (hydraulic, microCT, optical), pressure (P10, P50, P75), stem age (1, 2 and 3) and a random repeated measures term for stems nested within pressure (JMP 13.2.1, SAS Institute, Cary, NC, USA). All possible interactions were examined. Assumptions of parametric statistics were tested and supported. Differences in K_s and K_{ts} were compared via ANOVA. The model included stem age, method (K_s or K_{ts}) and the interaction. We used maximum values (emboli removed) for this analysis. Age differences were compared via pre-planned contrasts. Vessel diameter was analyzed via one-way ANOVA. For the benchtop dehydration method, for 3-year-old stems, we found that in some cases there was about 30% PLC_h and 20% PLC_t in hydrated stems (at or less negative than the predawn water potential values). Using microCT, we were able to determine that most emboli were present in the 2-year-old growth ring among the large early-wood vessels from the previous year of growth (Figure 1f). These vessels likely embolized in the previous year or over winter and were not functional at the time of our sampling. We corrected conductivity by subtracting out this initial embolism value (%) from all hydrated samples with this pattern (four benchtop samples and two microCT samples) to correct for initial native PLC as in Wang et al. (2014). Care was taken to make corrections for initial native-state embolism in a similar manner across all three methods so that comparisons across methods would not be confounded.

The relationship between K_s and K_{ts} was analyzed by computing slopes from standardized major axis regression models and 95% CIs. Data were broken into three categories that were low embolism (PLC = 0–20%), moderate embolism (PLC = 21–50%) and high embolism (PLC >50%).

The relationship between PLC_h and PLC_t was analyzed by computing slopes from standardized major axis regression models and 95% CIs. The relationships for the 2- and 3-year-old stems were linear, but the 1-year stems were not; therefore, only the linear portion of the curve was analyzed.

Results

Water status of plants

The studied plants were hydrated during our sampling. The mean (max, min, standard deviation) predawn water potentials (Ψ_{pd}) for branchlets that were bagged overnight were −0.41 (−0.34, −0.46, 0.05), −0.50 (−0.43, −0.53, 0.04), and −0.70 (−0.65, −0.74, 0.04) MPa for Plants 1, 2 and 3, respectively. For these same plants, not bagged overnight, Ψ_{pd} was more negative: −0.76 (−0.39, −1.20, 0.43), −0.95

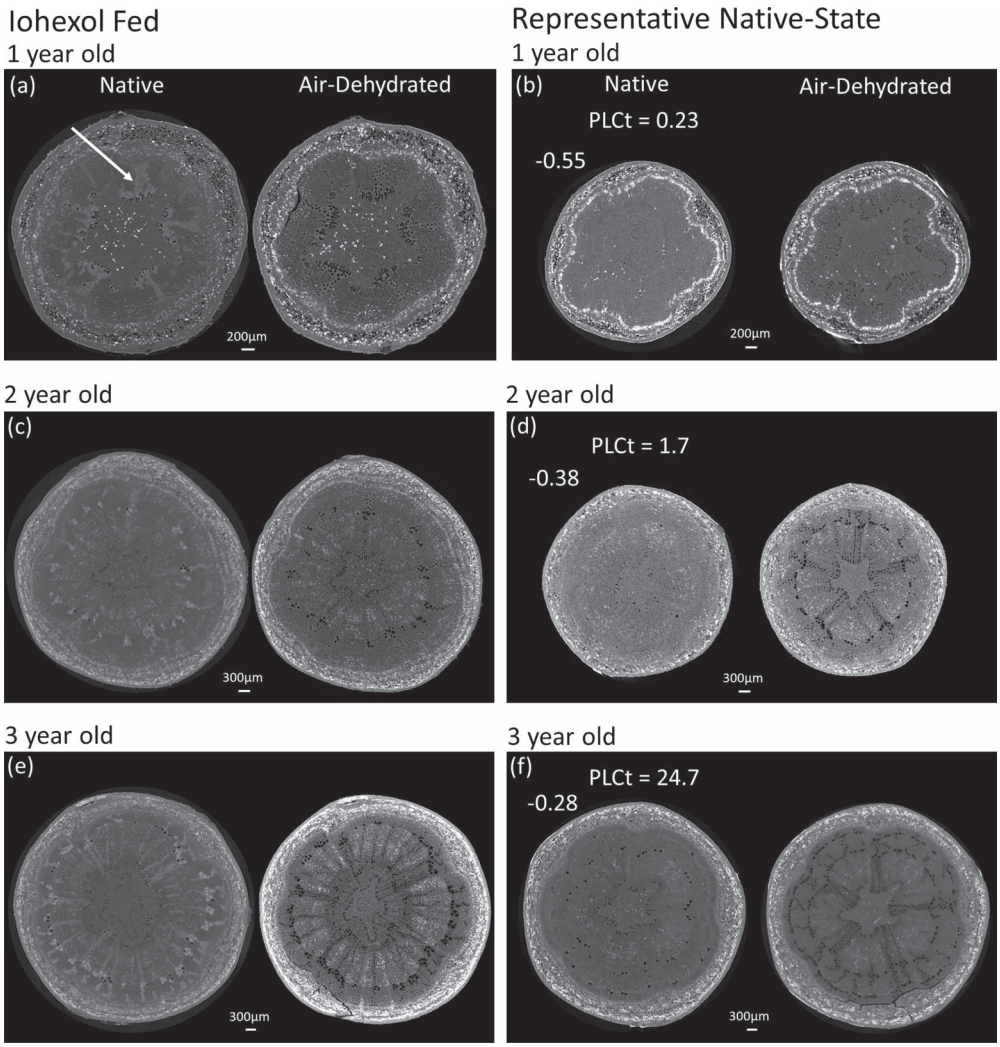

Figure 1. Example of microCT sections of hydrated stems fed with iodine to identify sap flow patterns (a, c, e) and examples of native embolism patterns without iodine (b, d, f). Within panels, left-side sections are the native state and right-side sections have been dehydrated by injecting conduits with dry gas. Functional sap pathways can be seen as white groups of conduits or bands of white conduits (arrow in a). The bright white dots seen in the pith, bark and portions of xylem are X-ray absorbing crystals. Dark conduits are filled with gas (embolized). The theoretical percentage loss of conductivity (PLC_t) is shown in c, d and f, as is the pressure potential of stem xylem (MPa).

(−0.76, −1.13, 0.18) and −1.65 (−1.40, −1.79, 0.21) for Plants 1, 2 and 3, respectively. The bagged Ψ_{pd}, which yields an estimate of stem pressure potential, indicated that the trees did not have significant water deficits during this very hot and dry time of year, which is consistent with plants being irrigated every morning. Moreover, the more negative unbagged Ψ_{pd} indicated nighttime transpiration.

Function and structure of xylem across stem age classes

Feeding iohexol into stems allowed us to identify which conduits were actively transporting sap (Figure 1). For 1-year-old stems, the xylem was functional all the way out to the cambium (Figure 1a), which is consistent with the presence of set buds and cessation of growth for the year. For two-year-old stems (Figure 1c), the first and second years of xylem were both moving sap and, for 3-year-old stems (Figure 1e), the third and second years were functional, but not the first. Thus, stems maintained sap transport in the two most recently produced growth rings (Figure 1c and e). In 3-year-old stems, the first-year xylem was not highly embolized, with the exception of the primary xylem, but it was not moving sap (Figure 1e). The presence of abundant vasicentric tracheids can be inferred from the bands of white iohexol in the images, and they interconnect the vessels creating an integrated network present in all three age classes (Figure 1a, c and e). In the 2- and 3-year-old stems (Figure 1c and e), at growth ring boundaries and near large earlywood vessels, the iohexol appears to be continuous across the growth ring suggesting inter-conduit connections that permit the movement of sap across rings.

Table 1. Vessel diameter statistics for different aged stems.

Age	*n*	Mean diameter (μm)	SE	SD	Min	Max
1-year old[A]	12	16.38	0.27	0.92	10.09	40.17
2-year old[B]	19	21.96	0.88	3.85	10.14	75.88
3-year old[B]	12	28.13	2.23	7.73	10.46	90.01

Different letters denote significant differences among the age groups.

Table 2. Maximum (in the absence of embolism) hydraulic stem specific conductivity (K_s) or theoretical stem specific conductivity (K_{ts}) for stems that differ in age.

Variable	K_s or K_{ts} (kg s^{-1} MPa^{-1} m^{-1})	SE	Min	Max
Hydraulic K_s				
1-year-old[A]	0.10	0.01	0.02	0.23
2-year-old[B]	0.63	0.09	0.08	1.41
3-year-old[C]	1.58	0.24	0.22	3.84
MicroCT K_{ts}				
1-year-old[A]	0.19	0.02	0.09	0.31
2-year-old[B]	1.11	0.14	0.18	2.76
3-year-old[C]	2.20	0.38	0.88	5.17
Method means				
Hydraulic[A]	0.77	0.08	0.02	3.84
MicroCT[B]	1.17	0.10	0.09	5.17

Different letters denote significant differences among the age groups within K_{ts} or K_s or across the different methods (K_s and K_{ts}).

Vessel anatomy changed with age. The first-year growth was diffuse porous (Figure 1a and b) and contained many isolated vessels with narrow diameters with a low variability among vessel diameters, i.e., low standard deviation (Table 1). By Year 2, some samples had xylem that was ring-porous, and the large earlywood vessels were much more connected than the first-year vessels (Figure 1c and d; Table 1). Samples were mixed in the degree that second-year xylem was ring porous; some of this variability is apparent when comparing across the different-aged samples in Figure 1. Year 3 samples always contained at least 1 year of ring-porous xylem, and many had two (Figure 1f). These differences in vessel diameters and porosity corresponded to significant increases in K_s and K_{ts} with stem age (Tables 1 and 2). Vessel length also increased with stem age. Mean (± 1 SE) vessel length (silicone injection method) of 1-year-old samples was 5.03 cm ± 0.92, 11.08 cm ± 1.32 for 2-year-old, and 15.45 cm ± 1.85 for 3-year-old (n = 6 for each age).

Vessel lengths are important in the context of methods. For sampling branches, we found that 3-year-old stems had an average maximum vessel length of 0.97 m (air-injection maximum values ranged from 1.29 to 0.40 m across samples, n = 5). One- and 2-year-old stems were not measured because we assumed that the 3-year-old samples were the longest and they would be closest to the cut branch base when harvesting branches.

Spatial context of embolism in hydrated stems

MicroCT images yield spatial information to examine embolism patterns. In their hydrated/native state, 1-year-old stems had little embolism, with only occasional emboli present within the primary xylem (Figure 1a and b). In 2- and 3-year-old stems, the primary xylem of the 1-year growth ring was typically embolized (Figure 1c–f). Moreover, when hydrated, these samples had a limited amount of embolism (Figure 1c and d). In some of the 3-year-old samples, the native state embolism level was estimated to be around 25% with microCT, which was chiefly due to embolism in the earlywood ring-porous vessels of the 2-year-old ring (Figure 1f). For the sample in Figure 1f, the embolized conduits of the 2-year-old growth ring contributed most to the estimated loss in conductivity. For the PLC_t reported for the sample (24.7%), 17% was due to embolized conduits in the previous growth rings, the vast majority of which were the 2-year-old earlywood vessels. The 1-year-old growth ring contributes very little to K_t because the conduit diameters are narrow (Eq. (1), Tables 1 and 2).

Estimates of vulnerability to embolism across methods and age classes

Vulnerability to embolism was assessed using three different methods and on three different-aged stems. All methods differed somewhat, but the patterns among the different-aged stems were similar. For the hydraulic method, none of the different aged stems was significantly different (Figure 2a; Table 3). For the microCT method, the 1-year-old stems were the most resistant to embolism compared with the 2- and 3-year-old stems, and the two older stems classes were not different (Figure 2b; Table 3). For the optical method, the 1-year-old stems were more resistant than the 3-year-old ones (Figure 2c; Table 3). These differences between the methods across the different ages were not great enough to lead to a significant interaction between method-type and age ($F_{4,8}$ = 1.279, P = 0.3543).

We also expressed the vulnerability to embolism for the hydraulic and microCT methods as losses in K_s and K_{ts} in response to xylem pressure potential (Figure S2 available as Supplementary Data at *Tree Physiology* Online). These curves show predicted and expected declines as pressure potential becomes more negative, and they also highlight the large differences in K_s and K_{ts} across the different age classes (Figure S2 available as Supplementary Data at *Tree Physiology* Online).

For the hydraulic method, cut stems were 14 cm long. This corresponds to an average of 0.97, 8.21 and 16.21% of open vessels in 1-, 2- and 3-year-old stems, respectively. None of the different-aged stems was significantly different in the resistance to embolism (Figure 2a; Table 3), despite the differences in

Table 3. Comparisons of mean vulnerability to embolism estimates of different aged stems and using three different methods (LCL and UCL are the lower and upper 95% confidence limits, respectively)

Variable	P10	LCL	UCL	P50	LCL	UCL	P75	LCL	UCL
Hydraulic PLC									
1-year-old^{A}	−1.33^{A}	−0.51	−3.00	−3.22^{A}	−2.39	−3.75	−4.45^{AB}	−3.72	−5.62
2-year-old^{A}	−0.99^{A}	−0.47	−2.26	−3.07^{A}	−2.47	−3.67	−4.65^{A}	−3.93	−5.80
3-year-old^{A}	−0.50^{A}	−0.22	−1.36	−2.19^{B}	−1.62	−2.88	−3.78^{B}	−3.01	−4.64
MicroCT PLC									
1-year-old^{A}	−3.86^{A}	−3.10	−4.20	−6.46^{A}	−6.25	−8.51	−7.82^{A}	−7.48	−11.70
2-year-old^{B}	−0.79^{B}	−0.33	−1.58	−4.40^{B}	−3.74	−6.15	−8.31^{A}	−6.24	−15.99
3-year-old^{B}	−0.92^{B}	−0.64	−1.51	−3.67^{B}	−2.30	−5.02	−6.10^{A}	−5.42	−9.56
Optical adj.									
1-year-old^{A}	−2.00^{A}	−0.82	−3.17	−5.60^{A}	−4.42	−6.77	−6.07^{A}	−4.89	−7.24
2-year-old^{AB}	−2.19^{B}	−1.01	−3.36	−3.77^{B}	−2.59	−4.94	−5.03^{A}	−3.85	−6.20
3-year-old^{B}	−0.89^{AB}	0	−2.06	−3.54^{B}	−2.36	−4.71	−5.54^{A}	−4.37	−6.72
Method									
Hydraulic^{A}	−0.94^{A}	−0.01	−1.88	−2.63^{A}	−1.68	−3.57	−4.29^{A}	−3.34	−5.23
MicroCT^{B}	−1.85^{A}	−0.93	−2.77	−4.84^{B}	−3.62	−5.77	−7.44^{B}	−6.52	−8.36
Optical^{C}	−1.69^{A}	−0.80	−2.57	−4.30^{B}	−3.41	−5.18	−5.54^{C}	−4.66	−6.43

P10 = the xylem pressure potential at 10% loss of hydraulic conductivity (measured and theoretical) or of total observed optical events, P50 = the same at 50% and P75 = the same at 75%. Within a method, values with different letters are significantly different as are the different age groups. In the left column, letters on the age labels compare the main effect of age within a method, and letters on method compare the main effect of method.

vessel length and the proportion of open vessels across the different ages.

Different methods produced different estimates of embolism resistance ($F_{2,8}$ = 20.703, P < 0.001). The microCT method produced the most resistant to embolism estimates, the optical method was intermediate and the hydraulic method produced the most vulnerable estimates (Table 3). There were no significant interactions among variables in the model (Table 3).

Measured and theoretical conductivity compared

Measured and theoretical conductivity were compared to understand key patterns in the data sets. Theoretical conductivity values were higher than measured K_s (Table 2; Figure 3). Moreover, we found that as stems experienced greater levels of embolism, the measured K_s increasingly deviated from K_{ts} (Figure 3). The relationship between PLC_h and PLC_t was not consistent across the different stem ages. The 1-year-old stems had a greater slope of PLC_h plotted against PLC_t indicating that small levels of embolism (PLC_t) were associated with larger K_h losses than was the case for the 2- and 3- year-old stems (Figure 4).

Testing for methods artifacts

Cutting artifacts can lead to overestimates of vulnerability to embolism using hydraulic methods. We tested for artifacts and found that stems cut under tension (−2.41 and −2.91 MPa) did not differ from stems that had their xylem tension relaxed (−0.20 and −0.23 MPa; Figure S3 available as Supplementary Data at *Tree Physiology* Online). Moreover, some hydrated 3-year-old stems (xylem pressure >−0.40 MPa) had embolism levels between 20 and 46% (Figure 1f); thus, this embolism cannot be attributed to a cutting artifact.

We tested for an additional cutting artifact. Hydraulic estimates of embolism were higher than those for microCT, and this was most pronounced for 1-year-old stems and at more negative xylem pressures (Figure 2; Figure S4b available as Supplementary Data at *Tree Physiology* Online). All of our microCT measures were done some distance (>4 cm) away from cut ends; thus, it was possible that air bubbles directly at the cut ends could lead to greater estimates of embolism in the hydraulic data compared to the microCT. We analyzed this by examining the embolism in the cut ends and centers of stems by scanning all three regions with microCT and found no significant differences for PLC_t or K_{ts} (Figure S4 available as Supplementary Data at *Tree Physiology* Online; $F_{1,4}$ = 1.743, P = 0.257 for PLC_t; $F_{1,4}$ = 3.677, P = 0.127 for K_{ts}). This indicates that gas blockages at the stem ends cannot explain the higher PLC for hydraulic measurements compared to microCT.

For many samples, we measured K_h after microCT scanning; thus, it was possible that the elevated PLC of hydraulic measures could be triggered by X-rays. We tested for this artifact in two ways. First, we analyzed PLC and K_s of stems that had been scanned three times and hydraulic conductivity was measured before and after the triple-scan. The PLC and K_s before and after the scans was not significantly different (Figure S5 available as Supplementary Data at *Tree Physiology* Online; t_2 = 1.177, P = 0.360 for PLC; t_2 = 1.226, P = 0.345 for K_s). Second, we compared hydraulic vulnerability curves generated on stems that had not been scanned to curves generated using stems that had been scanned. We found that the two curves were

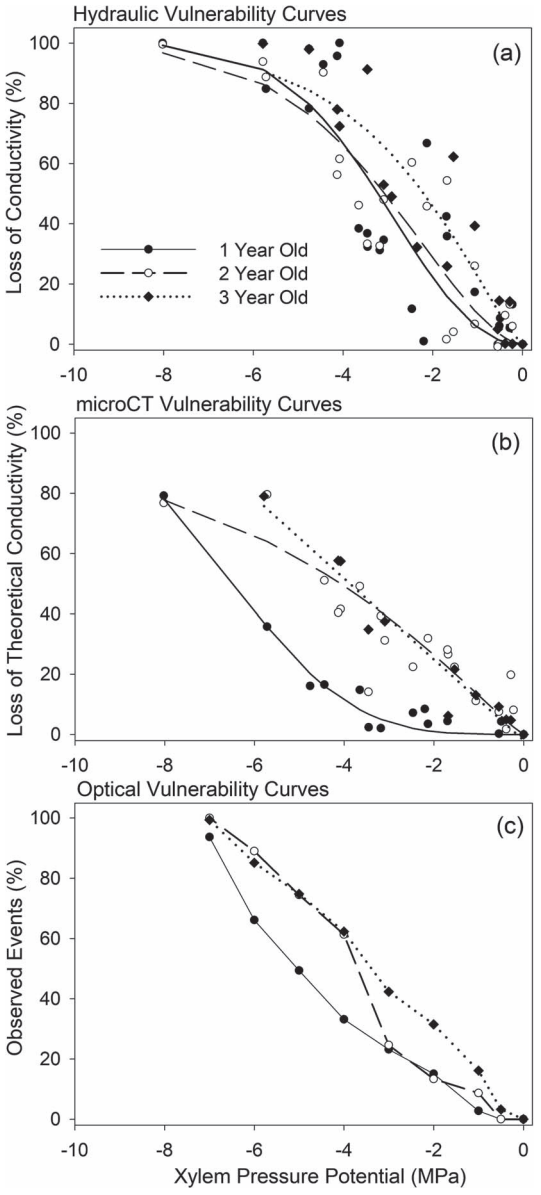

Figure 2. Vulnerability to embolism curves for stems of three different ages and using three different methods. Each data point represents a different stem in (a) and (b) (see Figure S2 available as Supplementary Data at *Tree Physiology* Online for curves expressed as specific conductivity), and three stems were measured using the optical method and the results were averaged to produce the curves shown in (c) (optical curves from each sampled stem are shown in Figure S1 available as Supplementary Data at *Tree Physiology* Online).

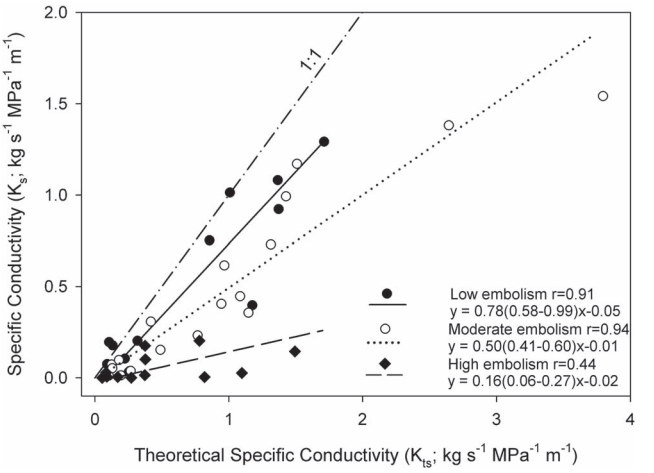

Figure 3. Measured specific conductivity (K_s) plotted in relation to theoretical specific conductivity (K_{ts}). Stems were categorized as low embolism (0–20% PLC), moderate embolism (21–50% PLC) and high embolism (>50% PLC). Theoretical conductivity values were greater than K_s values with increasing deviations as stems were more embolized. Linear equations are shown from standardized major axis regression where the values following the slopes in parentheses are the upper and lower 95% confidence limits (CLs). There was no overlap in CLs for slopes so significant differences in slopes are as follows: low embolism > moderate embolism > high embolism. The slope for all groups was significantly lower than 1.

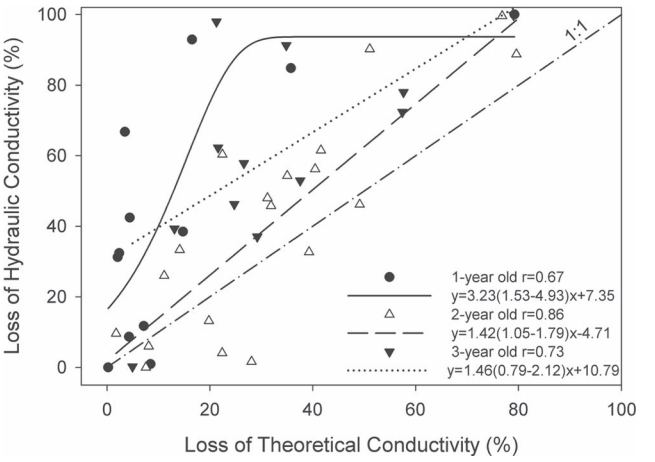

Figure 4. Measured loss of hydraulic conductivity (PLC_h) using the benchtop-hydraulic method plotted in relation to theoretical loss in conductivity (PLC_t) estimated using microCT. Linear equations are shown from standardized major axis regression where the values following the slopes in parentheses are the upper and lower 95% confidence limits (CL). Only the linear portion of the 1-year-old curve was analyzed, and all regressions were significant ($P \leq 0.018$). The slope of the 1-year-old stems was greater than the two older ones as the slopes fall outside the 1-year-old slope CL.

not significantly different (Figure S6 available as Supplementary Data at *Tree Physiology* Online ; P50 = −3.47 for non-scanned and −3.48 MPa for scanned).

Other artifacts that can occur with hydraulic measurements are clogging due to wounding that can lead to irreversible declines in the conductivity of stems, and refilling of embolized conduits. We measured K_s before and after the scans, a period of about 45 min, and the values were not different (Figure S5a and b available as Supplementary Data at *Tree Physiology* Online). This suggests that stems were neither clogging nor refilling. Moreover, when we flushed these stems to remove emboli, values went up as would be expected (Figure S5a available as Supplementary Data at *Tree Physiology* Online), suggesting that the PLC was primarily due to the presence of

emboli and not clogging (Figure S5b available as Supplementary Data at *Tree Physiology* Online).

Discussion

A comparison of two 'reference' methods: benchtop dehydration and microCT

There is currently no consensus regarding the best method to measure vulnerability to embolism in plants. The benchtop-hydraulic method and microCT imaging have both been argued to produce reliable results (Cochard et al. 2013, 2015). Here we tested these two methods and found that they did not agree. The microCT method produced curves that were significantly more resistant to embolism than the hydraulic method (Jacobsen et al. 2019, Venturas et al. 2019). Each of these methods is potentially susceptible to different errors in measurements and interpretation.

For the benchtop-hydraulic method, artifacts associated with the introduction of air into cut stems could artificially inflate vulnerability estimates. We carefully tested for this in our hydraulic methods, using best practices (Torres-Ruiz et al. 2015, Venturas et al. 2016). We also tested for other potential artifacts, including stem wounding, clogging, refilling and damage due to X-rays. We found no evidence that our hydraulic measures were affected by any of these potential known artifacts.

Another potential artifact is that long vessels can affect K_h measurements by increasing K_h if a sap-filled vessel is open through a sample (Brodribb et al. 2002, Chiu and Ewers 1993, Sperry et al. 2005). Few studies have examined this, and the patterns observed across species are variable (Jacobsen et al. 2015, Sperry et al. 2005). The effect of open vessels on K_h is partially mitigated because vessel K_h is affected by multiple traits beyond vessel ends including their lumens and perforation plates, which likely explains why a significant open vessel effect on K_h is generally not observed until many vessels are open (>40%; Sperry et al. 2005). If the long vessels with wide diameters are the ones more vulnerable to embolism, then sampling segments with more open vessels could lead to artificially low estimates of embolism resistance. However, the available data do not support this. Choat et al. (2010) found that hydraulic embolism measurements in grapevine stems made on long stem segments with no open vessels were not significantly different from measurements made on short segments. In the present study, 1-, 2- and 3-year-old stems differed in vessel length, yet they did not significantly differ in resistance to embolism using the conductivity method. We conclude that a vessel-length-conductivity artifact is an unlikely explanation for why the benchtop dehydration method disagrees with microCT.

The microCT method of estimating embolism resistance relies on the calculation of K_{ts} using the Hagen–Poiseuille relationship to estimate hydraulic function based on vessel diameter. This relationship makes several assumptions that are violated by xylem conduits. One assumption is that sap is flowing through ideal conduits of a constant and circular diameter. This assumption is violated by xylem conduits in several ways, including the presence of pits and pit membranes (Schulte et al. 1987). This is why estimates of K_{ts} are generally greater than those of K_s (Schulte et al. 1987, Nolf et al. 2017). Furthermore, the microCT method assumes that this divergence of conduits from Hagen–Poiseuille assumptions remains constant as emboli occur. Our data suggest that this assumption is invalid. This likely occurs because pathways for sap to flow become more limited when emboli are present, leading to increased disparity between actual conductivity and Hagen–Poiseuille estimates as sap must traverse increasing numbers of pits and the overall pathway lengthens (Jacobsen and Pratt 2018, Mrad et al. 2018). The hydraulic method directly measures K_h, which integrates the resistances of the xylem vessel network, and this is likely why the microCT method underestimates K_h losses when compared with the benchtop-hydraulic method.

Previous comparisons between benchtop-based hydraulic and microCT data are few, and they generally support the results of this study. Nolf et al. (2018) compared these methods in a *Eucalyptus* sp. and found that the PLC_t did not exceed 80%, whereas PLC_h went to near 100%, a result similar to ours. Similarly, a study on *Populus trichocarpa* found that PLC_h was near 100% when PLC_t was only around 50%, a large difference that may be due to the diffuse porous xylem and very short vessel lengths in this species (Jacobsen et al. 2019, Venturas et al. 2019). One study observed lower estimates of embolism resistance for microCT than hydraulic methods for an herb, and this may be due to the damaging effects of X-rays on sensitive herbaceous tissue (Petruzzellis et al. 2018, Savi et al. 2017). Cochard et al. (2015) compiled hydraulic data and compared it with microCT for *Laurus nobilis* and found that the microCT estimates indicated much greater resistance to embolism. Finally, in an exception to these other studies, Losso et al. (2019) found good agreement between microCT and hydraulic estimates for embolism resistance measured on seedlings of two temperate tree species (see also Nardini et al. 2017). There are numerous reasons why methods comparisons may differ among studies, and this provides fodder for future studies (Hacke et al. 2015, Nardini et al. 2017, Pratt and Jacobsen 2018).

We conclude that the use of microCT as a reference method is fraught with potential errors. Direct measurement of xylem function through hydraulic methods provides information that microCT analyses are not yet able to accurately estimate.

The optical method compared to the benchtop-hydraulic method

The optical method overestimated embolism resistance compared to the hydraulic method. Methods that only measure counts of events (optical method or acoustic methods) assume

that each event has an equivalent effect on conductivity (Brodribb et al. 2017, Jackson and Grace 1996). This assumption is almost certainly invalid, as angiosperm vascular systems are commonly comprised of conduits with a wide range of conduit diameters that contribute differently to K_s (Eq. (2); Brodribb et al. 2017). Tracheid-based systems may reasonably approximate this assumption in some cases (Brodribb et al. 2017, Tyree and Dixon 1986). In this study, the 1-year-old stems were diffuse porous and relatively short vesselled, which is the best-case scenario for the optical method; however, all stem ages, regardless of porosity, similarly diverged between hydraulic and optical methods.

The optical method underestimated embolism resistance in cottonwood (*Populus trichocarpa*; Venturas et al. 2019). This result was linked to xylem fibers that were damaged in the debarked region where the optical data were collected, and the damage apparently created spurious (non-vessel) optical events that led to an overcounting of vessel embolism events (Venturas et al. 2019). Brodribb et al. (2017) also found that embolism resistance from the optical method significantly underestimated that from a hydraulic method in rosemary (*Rosmarinus officinalis*), which is also consistent with damage.

The present study found that the optical method overestimated embolism resistance in oak stems. In stems, the optical method only samples a small portion of the outer xylem tissue, which in our study will contain the latewood conduits. It is possible that these latewood conduits, including abundant tracheids, are an unrepresentative sample and are more resistant to embolism and contribute less to conductivity than other regions of the xylem such as the earlywood. The hydraulic method will integrate across the early and late wood, and primary xylem, which may explain why the optical method overestimates resistance for this oak. There are six published data sets comparing the optical method in stems to an independent hydraulic method (Brodribb et al. 2016, Venturas et al. 2019, and this study) and, of these, only one of the six samples shows agreement. The data suggests that the optical method applied to angiosperm stems is limited for accurately predicting conductivity losses.

Embolism resistance of oaks

Skelton et al. (2018) recently reported a P50 value for 1-year-old stems of *Q. douglasii* of −6.27 MPa using the optical method. They sampled a different population from the one we sampled; nevertheless, their P50 is not significantly different from what we found for 1-year-old stems with this same method. This means that any intraspecific differences between oak populations or differences in the way we implemented the method are likely minimal and that our results with the optical method are comparable to theirs.

While our P50 values did not differ, our curves do differ in detecting optical events at relatively high (less negative) pressure potentials. One explanation for this is that Skelton et al. (2018) sampled in a way that artificially introduced embolism. We sampled our plants at dawn; our plants were hydrated and kept so prior to sampling. By contrast, Skelton et al. (2018) did not sample hydrated plants, did not immerse the cut ends in water and had a much longer transit time prior to sampling than we did. Thus, the most vulnerable vessels likely embolized before they began their measurements, creating an artificial appearance of no embolism in the early portion of the curve. Even though they rehydrated their branches in the lab, this was unlikely to refill embolized conduits in oaks (Tobin et al. 2013).

Skelton et al. (2018) suggested that oaks were more embolism-resistant than previous studies had suggested and that avoidance of embolism in stems was an important aspect of their drought tolerance. Based on our analyses, this conclusion is likely driven by the optical method they used. The benchtop-hydraulic method used here does not support their findings for *Q. douglasii*. Because of the possibility of at least two different artifacts associated with the optical method, comparing across species with this technique is likely to be problematic.

One interesting anatomical feature of oaks is their abundant vasicentric tracheid network (Carlquist 1985, Pratt and Jacobsen 2015). Oaks commonly maintain positive stomatal conductance even at quite negative water potentials (Baldocchi and Xu 2007, Welker and Menke 1990, Xu and Baldocchi 2003), which likely relates to the tracheids. When vessels embolize, the extensive tracheid network can move sap around embolized vessels. This network is visible in the iohexol fed stems in Figure 1a, c and e. The argument made by Skelton et al. (2018), that oaks avoid embolism, does not accord with the hypothesis that the role of tracheids is to allow oaks to function when vessels embolize (Carlquist 1985).

Advanced vegetation models aim to predict future species distributions in the context of warmer and drier climates by using vulnerability to embolism curves. If inaccurate curves are used in such models, then model predictions will be misleading. The curves produced by Skelton et al. (2018) will overestimate the ability of oaks to tolerate a warming and drying climate. This is not a small overestimate: the P50 reported by Skelton et al. (2018) is −6.27 and our optical P50 = −5.61. These values are significantly more negative than the benchtop P50 (−3.22 MPa) found here. *Quercus douglasii* has suffered significant mortality during recent droughts in California (Brown et al. 2018), indicating that they are under threat from climate change-type droughts and that such a threat should not be underestimated.

Reliable estimates of stem xylem pressure potentials are needed to understand oak drought resistance. Significant nighttime transpiration in this species (Fisher et al. 2007) means that the measured predawn water potential will be more negative than the stem pressure potential (Donovan et al. 2003). Thus, it is not clear how negative the stem xylem pressure potentials

regularly are in the field for *Q. douglasii* and more measurements of bagged and equilibrated samples are needed.

Differences in embolism resistance across different aged xylem and the 'real' vulnerability curve

The benchtop-hydraulic method did not differ across the three ages, whereas the older stems were more vulnerable with the other two methods. Comparing data from microCT and the hydraulic method provides insights into these differences. The 1-year-old stems had a steeper slope when comparing PLC_h with PLC_t. This means that 1-year-old stems experience greater K_h declines for a given number of vessels blocked by emboli. This likely relates to the anatomy of the diffuse porous 1-year-old xylem that had vessels that were more isolated, narrower in diameter, and vessels that were shorter in length compared with older xylem. When a short and isolated vessel undergoes embolism, the pathways for sap to move around the non-functional conduit are more limited and K_h at the tissue level will decline more rapidly than a more connected network with longer vessels, which is represented by the 2- and 3-year-old earlywood (Jacobsen and Pratt 2018, Mrad et al. 2018). Nolf et al. (2018) also found greater resistance in 1-year-old stems using microCT.

It is challenging to measure vulnerability to embolism curves on stems ≥2 years old; however, it is important that such tissues be studied. Older xylem and larger branches may be important in determining drought resistance of large and long-lived plants (Fukuda et al. 2015, Nolf et al. 2017). One challenge is knowing which of the older rings are functional (Ellmore and Ewers 1986), which we determined using iohexol as a tracer. We found that sap was moving through the vessels and tracheids of two most recent growth rings within our sampled trees. This pattern is likely possible because our region often has mild winters, so freeze/thaw-induced embolism may be rare. Iohexol was present in conduits at growth ring boundaries and appeared to form a continuum across growth rings. In oaks, the presence of tracheids (vascular and vasicentric) may be a common pathway whereby sap can cross a growth ring through inter-conduit connections. Studies of pits in tracheids at growth ring boundaries would be useful in this context (Kitin et al. 2009).

Based on our tracer data, for 3-year-old stems of *Q. douglasii*, the most functionally relevant approach to quantify the 'real' vulnerability curve would be to only sample the two most recent growth rings. For 2-year-old stems, it would be most relevant to measure all of the xylem in the 1- and 2-year-old-age classes as we did here. When using hydraulic methods on cut stems, solution is pushed through sapwood of all ages, provided that there are no permanent occlusions such as tyloses. For hydraulic methods, non-functional rings could be sealed with glue to block flow through those that are non-functional (Rodriguez-Zaccaro et al. 2019). Here, errors associated with including the oldest growth ring were likely small because 1-year-old xylem contributed very little to overall K_s and K_{ts}. As stems get older than 3 years, the vulnerability curve that most closely approximates the 'real' in vivo curve may diverge from ones that measure older non-functional growth rings in addition to the newest and active ones.

Debate has focused on cutting and long vessels to explain discrepancies and artifacts among methods (Cochard et al. 2015), yet age-associated effects, particularly based on the number, inclusion and function of older growth rings, are potentially more important factors in explaining differences across studies that have differed in the ages of their sampled material (Cochard et al. 2013, Hacke et al. 2015). Often, such age-effects are referred to as 'fatigue effects', where fatigued conduits are ones that embolize and become damaged, thereby reducing their embolism resistance after they are refilled (Hacke et al. 2001); however, simply referring to older xylem as suffering from 'fatigue effects' masks a more complex and interesting set of questions that arise when sampling older stems. New methods and combined approaches make it easier than ever to measure embolism resistance and the functional contribution of older stems accurately and informatively.

Summary

The standard hydraulic method used on benchtop dehydrated samples was found to be a reliable method that can be implemented in a manner that avoids hypothesized errors associated with sampling and provides information on the hydraulic conductivity of complex xylem tissue. The microCT method can effectively detect the presence of emboli, but accurately translating the presence of emboli to conductivity is currently not possible. For K_{ts} to closely approximate K_s, K_{ts} estimates must account for how embolism interacts with the 3D hydraulic network (Jacobsen and Pratt 2018, Mrad et al. 2018). The optical method did not agree with either the hydraulic or the microCT method, and it is not able to predict theoretical conductivity or gather information on the distribution and sizes of embolized conduits; thus, that method is not recommended for the sampling of angiosperm stems. Like the microCT method, solely relying on the optical method is not advised if the goal of a study is to represent resistance to embolism in a way this is most relevant to plant physiology and drought resistance. Combining hydraulic and microCT methods is a powerful approach and, when coupled with an anatomically informed model, like the one by Mrad et al. (2018; see also Schulte et al. 1987), represents a promising way forward for future research.

Supplementary Data

Supplementary Data for this article are available at *Tree Physiology* Online.

Acknowledgments

Martin Venturas kindly provided the R-script used to calculate confidence limits for some vulnerability curves.

Funding

The Department of Defense Army Research Office award No. 68885-EV-REP (R.B.P.) is gratefully acknowledged. NSF CREST grant HRD-1547784 (R.B.P. and A.L.J.) and Career Grant IOS-1252232 (A.L.J.) are acknowledged for support.

Conflict of Interest statement

None declared.

References

Baldocchi DD, Xu L (2007) What limits evaporation from Mediterranean oak woodlands–the supply of moisture in the soil, physiological control by plants or the demand by the atmosphere? Adv Water Resour 30:2113–2122.

Brodribb T J, Holbrook NM, Gutierrez MV (2002) Hydraulic and photosynthetic co-ordination in seasonally dry tropical forest trees. Plant Cell Environ 25:1435–1444.

Brodribb TJ, Carriqui M, Delzon S, Lucani C (2017) Optical measurement of stem xylem vulnerability. Plant Physiol 174:2054–2061.

Brown BJ, McLaughlin BC, Blakey RV, Morueta-Holme N (2018) Future vulnerability mapping based on response to extreme climate events: dieback thresholds in an endemic California oak. Divers Distrib 24:1186–1198.

Carlquist S (1985) Vasicentric tracheids as a drought survival mechanism in the woody flora of southern California and similar regions; review of vasicentric tracheids. Aliso 11:37–68.

Chiu ST, Ewers FW (1993) The effect of segment length on conductance measurements in *Lonicera fragrantissima*. J Exp Bot 44:175–181.

Choat B, Drayton WM, Brodersen C, Matthews MA, Shackel KA, Wada H, McElrone AJ (2010) Measurement of vulnerability to water stress-induced cavitation in grapevine: a comparison of four techniques applied to a long-vesseled species. Plant Cell Environ 33:1502–1512.

Cochard H, Delzon S, Badel E (2015) X-ray microtomography (micro-CT): a reference technology for high-resolution quantification of xylem embolism in trees. Plant Cell Environ 38:201–206.

Davis SD, Ewers FW, Pratt RB, Brow PL, Bowen TJ (2005) Interactive effects of freezing and drought on long distance transport: a case study of chaparral shrubs of. In: Holbrook CN, Zwieniecki M (eds) Vascular transport in plants. Academic Press, New York, NY:425–435.

Donovan LA, Richards JH, Linton MJ (2003) Magnitude and mechanisms of disequilibrium between predawn plant and soil water potentials. Ecology 84:463–470.

Ellmore GS, Ewers FW (1986) Fluid flow in the outermost xylem increment of a ring-porous tree, *Ulmus americana*. Am J Bot 73:1771–1774.

Fisher JB, Baldocchi DD, Misson L, Dawson TE, Goldstein AH (2007) What the towers don't see at night: nocturnal sap flow in trees and shrubs at two AmeriFlux sites in California. Tree Physiol 27:597–610.

Fukuda K, Kawaguchi D, Aihara T, Ogasa MY, Miki NH, Haishi T, Umebayashi T (2015) Vulnerability to cavitation differs between current-year and older xylem: non-destructive observation with a compact magnetic resonance imaging system of two deciduous diffuse-porous species. Plant Cell Environ 38:2508–2518.

Gilbert SG (1940) Evolutionary significance of ring porosity in woody angiosperms. Bot Gaz 102:105–119.

Greenidge KNH (1952) An approach to the study of vessel length in hardwood species. Am J Bot 39:570–574.

Hacke UG, Sperry JS, Pittermann J (2000) Drought experience and cavitation resistance in six shrubs from the Great Basin, Utah. Basic Appl Ecol 1:31–41.

Hacke UG, Stiller V, Sperry JS, Pittermann J, McCulloh KA (2001) Cavitation fatigue embolism and refilling cycles can weaken the cavitation resistance of xylem. Plant Physiol 125:779–786.

Hacke UG, Venturas MD, MacKinnon ED, Jacobsen AL, Sperry JS, Pratt RB (2015) The standard centrifuge method accurately measures vulnerability curves of long-vesselled olive stems. New Phytol 205:116–127.

Halis Y, Mayouf R, Benhaddy ML, Belhamra M (2013) Intervessel connectivity and relationship with patterns of lateral water exchange within and between xylem sectors in seven xeric shrubs from the great Sahara desert. J Plant Res 126:223–231.

Jackson GE, Grace J (1996) Field measurements of xylem cavitation: are acoustic emissions useful. J Exp Bot 47:1643–1650.

Jacobsen AL, Pratt RB (2012) No evidence for an open vessel effect in centrifuge-based vulnerability curves of a long-vesselled liana (*Vitis vinifera*). New Phytol 194:982–990.

Jacobsen AL, Pratt RB (2018) Going with the flow: structural determinants of vascular tissue transport efficiency and safety. Plant Cell Environ 41:2715–2717.

Jacobsen AL, Rodriguez-Zaccaro FD, Lee TF, Valdovinos J, Toschi HS, Martinez JA, Pratt RB (2015) Grapevine xylem development, architecture, and function. In: Hacke U (ed) Functional and ecological xylem anatomy. Springer-Verlag, New York, NY:133–162.

Jacobsen AL, Pratt RB, Venturas MD, Hacke UG (2019) Large volume vessels are vulnerable to water-stress-induced embolism in stems of poplar. IAWA J 40:4–22.

Kitin P, Fujii T, Abe H, Takata K (2009) Anatomical features that facilitate radial flow across growth rings and from xylem to cambium in *Cryptomeria japonica*. Ann Bot 103:1145–1157.

Kursar TA, Engelbrecht BM, Burke A, Tyree MT, Omari BE, Giraldo JP (2009) Tolerance to low leaf water status of tropical tree seedlings is related to drought performance and distribution. Funct Ecol 23:93–102.

Losso A, Bär A, Dämon B et al. (2019) Insights from in vivo micro-CT analysis: testing the hydraulic vulnerability segmentation in *Acer pseudoplatanus* and *Fagus sylvatica* seedlings. New Phytol 221:1831–1842.

Mackay DS, Roberts DE, Ewers BE, Sperry JS, McDowell NG, Pockman WT (2015) Interdependence of chronic hydraulic dysfunction and canopy processes can improve integrated models of tree response to drought. Water Resour Res 51:6156–6176.

Mrad A, Domec JC, Huang CW, Lens F, Katul G (2018) A network model links wood anatomy to xylem tissue hydraulic behaviour and vulnerability to cavitation. Plant Cell Environ 41: 2718–2730.

Nardini A, Savi T, Losso A et al. (2017) X-ray microtomography observations of xylem embolism in stems of *Laurus nobilis* are consistent with hydraulic measurements of percentage loss of conductance. New Phytol 213:1068–1075.

Nolf M, Lopez R, Peters JM, Flavel RJ, Koloadin LS, Young IM, Choat B (2017) Visualization of xylem embolism by X-ray microtomography: a direct test against hydraulic measurements. New Phytol 214:890–898.

Petruzzellis F, Pagliarani C, Savi T et al. (2018) The pitfalls of in vivo imaging techniques: evidence for cellular damage caused

by synchrotron X-ray computed micro-tomography. New Phytol 220:104–110.
Pratt RB, Jacobsen AL (2017) Conflicting demands on angiosperm xylem: tradeoffs among storage, transport and biomechanics. Plant Cell Environ 40:897–913.
Pratt RB, Jacobsen AL (2018) Identifying which conduits are moving water in woody plants: a new HRCT-based method. Tree Physiol 38:1200–1212.
Pratt RB, Jacobsen AL, Mohla R, Ewers FW, Davis SD (2008) Linkage between water stress tolerance and life history type in seedlings of nine chaparral species (Rhamnaceae). J Ecol 96:1252–1265.
Pratt RB, Percolla MI, Jacobsen AL (2015) Integrative xylem analysis of chaparral shrubs U Hacke. In: Hacke U (ed) Functional and ecological xylem anatomy. Springer-Verlag, New York, NY:189–207.
Rodriguez-Zaccaro FD, Valdovinos-Ayala J, Percolla MI, Venturas MD, Pratt RB, Jacobsen AL (2019) Wood structure and function change with maturity: age of the vascular cambium is associated with xylem changes in current-year growth. Plant Cell Environ 42: 1816–1831.
Rosell JA, Olson ME, Anfodillo T (2017) Scaling of xylem vessel diameter with plant size: causes, predictions, and outstanding questions. Curr For Rep 3:46–59.
Savi T, Miotto A, Petruzzellis F, Losso A, Pacilè S, Tromba G, Mayr S, Nardini A (2017) Drought-induced embolism in stems of sunflower: a comparison of in vivo micro-CT observations and destructive hydraulic measurements. Plant Physiol Biochem 1:24–29.
Schulte PJ, Gibson AC, Nobel PS (1987) Xylem anatomy and hydraulic conductance of *Psilotum nudum*. Am J Bot 74:1438–1445.
Skelton RP, Dawson TE, Thompson SE, Shen Y, Weitz AP, Ackerly D (2018) Low vulnerability to xylem embolism in leaves and stems of north American oaks. Plant Physiol 177: 1066–1077.
Sperry JS, Hacke UG, Wheeler JK (2005) Comparative analysis of end wall resistance in xylem conduits. Plant Cell Environ 28:456–465.
Tobin MF, Pratt RB, Jacobsen AL, De Guzman ME (2013) Xylem vulnerability to cavitation can be accurately characterised in species with long vessels using a centrifuge method. Plant Biol 15:496–504.
Torres-Ruiz JM, Jansen S, Choat B et al. (2015) Direct X-ray microtomography observation confirms the induction of embolism upon xylem cutting under tension. Plant Physiol 167:40–43.
Tyree MT, Dixon MA (1986) Water stress induced cavitation and embolism in some woody plants. Physiol Plant 66:397–405.
Venturas MD, MacKinnon ED, Jacobsen AL, Pratt RB (2016) Excising stem samples underwater at native tension does not induce xylem cavitation. Plant Cell Environ 38:1060–1068.
Venturas MD, Pratt RB, Jacobsen AL, Castro V, Fickle JC, Hacke UG (2019) Direct comparison of four methods to construct xylem vulnerability curves: differences among techniques are linked to vessel network characteristics. Plant Cell Environ 42:2422–2436.
Wang R, Zhang L, Zhang S, Cai J, Tyree MT (2014) Water relations of *Robinia pseudoacacia* L: do vessels cavitate and refill diurnally or are R-shaped curves invalid in Robinia? Plant Cell Environ 37:2667–2678.
Welker JM, Menke JW (1990) The influence of simulated browsing on tissue water relations, growth and survival of *Quercus douglasii* (Hook and Arn) seedlings under slow and rapid rates of soil drought. Functional Ecology 1:807–817.
Wheeler JK, Huggett BA, Tofte AN, Rockwell FE, Holbrook NM (2013) Cutting xylem under tension or supersaturated with gas can generate PLC and the appearance of rapid recovery from embolism. Plant Cell Environ 36:1938–1949.
Xu L, Baldocchi DD (2003) Seasonal trends in photosynthetic parameters and stomatal conductance of blue oak (*Quercus douglasii*) under prolonged summer drought and high temperature. Tree Physiol 23:865–877.